Standard Issue – Article

Journal of Agricultural Engineering

https://www.agroengineering.org/

An air-assisted mechanical hill-seeding device for foxtail millet (*Setaria italica*)

Lingxin Bu, Qianwen Kou, Adilet Sugirbay, Jun Chen, Yu Chen

Please cite this article as doi: 10.4081/jae.2024.1578

Submitted: 28/08/2023
Accepted: 11/12/2023

An air-assisted mechanical hill-seeding device for foxtail millet (*Setaria italica*)

Lingxin Bu,[1] Qianwen Kou,[1] Adilet Sugirbay,[2] Jun Chen,[3] Yu Chen[3]

[1]North Minzu University, Yinchuan, Ningxia, China; [2]Technical Faculty, S. Seifullin Kazakh Agro Technical University, Astana, Kazakhstan; [3]College of Mechanical and Electronic Engineering, Northwest A&F University, Yangling, China

Correspondence: Yu Chen, College of Mechanical and Electronic Engineering, Northwest A&F University, Yangling 712100, China.
Tel.: +86.02987091867.
E-mail: jdxy73@nwafu.edu.cn

Key words: foxtail millet (*Setaria italic*); hole forming device; precision seeding; quality index.

Acknowledgments: the work in this paper was supported by the National Key Research and Development Program (No.2018YFD0701102), the Natural Science Foundation of Ningxia (No. 2023AAC03302) and North Minzu University under grant agreement number 2021KYQD31. We thank LetPub (www.letpub.com) for its linguistic assistance during the preparation of this manuscript.

Conflict of interest: the authors declare no potential conflict of interest.

Abstract

Setaria italica **(**foxtail millet) plays an important role in human nutrition, animal feed, and agriculture. However, the difficulty in realizing precision seeding introduces challenges to the planting and industrialization of foxtail millet. To address the challenge of suboptimal seeding effects for foxtail millet seeds, we engineered an air-assisted mechanical foxtail millet hole seeder equipped with a duckbill hole-forming device. Through bench testing, we investigated the influence of the wire diameter of the return spring on the seeding effect, as well as the interactive effects of the vacuum pressure of the seed-metering device and the rotational speed of the dibber wheel on seeding performance. The results show the following. (1) With the return spring having a major diameter of 44 mm, minor diameter of 2 mm, and length of 70 mm, wire diameters of 1.4, 1.6, and 1.8 mm were evaluated for conformity with standard requirements for the quality index. Given the reduced tearing extent with a smaller wire diameter, a wire diameter of 1.4 mm was selected. (2) The vacuum pressure of the seed-metering device and the rotational speed of the dibber wheel had a significant impact on the quality index. Using the response surface methodology (RSM) for parameter optimization, we aimed to maximize the qualification rate and minimize the missing and double seeding rates. Optimal parameters were found with an inlet vacuum pressure of −7.8 kPa, a dibber wheel speed of 75 r/min, and a seeder forward speed of 1.69 m/s (6.08 km/h). These settings achieved a quality index of 89.88%, a multiples index of 1.56%, and a miss index of 8.56%, in accordance with model predictions. Field tests were conducted with the determined parameters, revealing that at a seeder forward speed of 1.67 m/s (6 km/h) and a metering device vacuum pressure of −7.8 kPa, the average seed spacing was 16.51 mm, the hole spacing coefficient of variation was 2.55%, the mean seeding quality index was 88.46%, and the seedling pass rate was 97.77%. Thus, the designed air-suction-assisted mechanical foxtail millet hole seeder complies with the standard requirements and represents an advancement in agricultural machinery for small grain crops.

Introduction

In recent years, the cultivation of coarse grains has come into focus as a means to confront the scarcity of water resources. *Setaria italic* (foxtail millet), a coarse grain crop with substantial drought resistance and tolerance to infertile conditions, has experienced a gradual expansion in its cultivation scale. However, difficulties in controlling foxtail millet seeding due to its small size have resulted in lower quality and yield in planting (Zhang *et al*., 2007).

With the mechanization of agriculture, mechanical row planting has become the primary method for small-seeded crop sowing. Row planters enable more precise control over row spacing and furrow depth. Moreover, by parameterizing key components such as furrowing and seeding based on the diverse cultivation requirements of different crops, growers can ensure various seeding technological demands affecting yield, thereby enhancing seeding uniformity, and operational efficiency. However, this seeding approach, which increases seedling emergence rates by augmenting seeding quantity, necessitates manual thinning after seed emergence, so labor costs remain substantial (Yang and Zhao, 2007).

Mechanical precision seeding, which is an improvement on mechanical row planting, has gradually gained traction for small seeds. This method goes beyond the agronomic requirements achievable by row planters, further controlling hole spacing and the number of seeds per hole and delivering a certain quantity of foxtail millet to pre-designed locations within the soil before seed covering. Seed-metering devices are key components ensuring seeding quality and can be classified into two types, mechanical precision seed-metering devices and air-suction seed-metering devices, based on the mechanical seed-picking and air-suction seed-picking principles, respectively (Cui *et al*., 2003). Mechanical precision seed-metering devices boast advantages such as a simple structure, easy manufacturability, and low production costs, and they can achieve good results at slower operating speeds. However, this may result in missed seeds and poor seed distance uniformity at high seeding speeds, thereby affecting yield (Parish, 1972). Conversely, air-suction seed-metering devices can achieve higher seeding quality at high operating speeds (Singh *et al*., 2005), but these devices require high chamber sealing, have a complex structure, are prone to wear, and their seeding quality depends entirely on air force. Moreover, issues such as air hole blockages, while rare, can severely impact seeding quality if they occur (Wan *et al*., 2019).

Exploration of mechanical seed-metering devices for small seeds has mainly focused on structural improvements to make them more suitable for the planting patterns of small seeds. Bian *et al*. (2007) designed a novel foxtail millet seed-metering device, adapting the shape of the seed slots on the grooved wheel to the specific physical characteristics of foxtail millet. This design allows the seeds to enter the designated slots in an orderly fashion and then be discharged through gravity. An additional high-frequency vibration system is included to shake the metering device, improving the filling quality. The design also features various seed discs with different shapes, allowing for selection based on the specific seeds. Zhang *et al*. (2010) introduced a new multifunctional seed-metering device for the precision seeding of small-seeded crops and further developed a novel precision seed-metering device with a mechanical structure to push seeds out of the metering device for various small-diameter seeds. The ground wheel was driven by friction and therefore provided power, while the periphery of the seeding wheel contained multiple rows of differently shaped filling belts. Inside the seeding wheel, a brush removes excess seeds, and a push-seed wheel meshes with the seeding hole to squeeze the seeds out, achieving sowing. Different combinations of seeding and push-seed wheels can be assembled according to different seeds. Xie and Liu (2018) addressed the poor seeding quality phenomenon experienced with small-seeded crops like foxtail millet and rapeseed when using a dimpled wheel seed-metering device for precision seeding. Bench tests were conducted using a dimpled wheel seed-metering device as the research subject to find the optimal working parameters for small-seeded crop sowing with the dimpled wheel seed-metering device, thereby providing new insights into its adaptation for the seeding of small-seeded crops.

The removal of seeds adhering to the air holes of pneumatic seed-metering devices through mechanical or pneumatic means has become a vital area of research for small-seeded pneumatic seed-metering, particularly the exploration of seed clearing methods for air holes (Li *et al*., 2016). Zhang *et al*. (2016) addressed the phenomenon of seeds easily adhering to air holes by adding a cleaning device to the pneumatic seed-metering system. This structure effectively cleared seeds adhering to the air holes, reducing the likelihood of clogging, but it did not fundamentally resolve the root problem of missed seeding in pneumatic seed-metering devices. Singh *et al*. (2005) analyzed the effect of the operational speed of the disc, vacuum pressure, and shape of the entry of the seed hole on seeding quality to optimize the design and operating parameters for cottonseed planting. Lower multiple indices were found at lower pressure and higher speeds, and operating at a linear speed of the seed-sowing disc from 0.34 to 0.44 m/s and a vacuum pressure of 2 kPa produced superior seeding results. Kang *et al*. (2020) employed a combination of pneumatic and mechanical methods to clear seeds adhering to the air holes, utilizing a partition plate structure to reduce the vacuum chamber's size and enhance seed-blowing efficiency. Furthermore, a mechanical seed-clearing device was designed to clear seeds stuck in the air holes. The test results showed a maximum qualification rate of 93.2%, exceeding the national standard qualification rate of at least 80%.

In summary, mechanical seed-metering devices can achieve satisfactory seeding results at lower working speeds but are unsuitable for higher-speed seeding operations. In contrast, pneumatic seed-metering devices rely on the vacuum size of the air chamber and can experience a drastic drop in seeding quality when clogging occurs. Pneumatic and mechanical composite seed-metering devices represent a new direction in seed-metering research. Accordingly, we designed a pneumatic-assisted mechanical foxtail millet hole seeder, and based on this, we conducted an experiment to determine its working parameters and complete its field seeding performance evaluation.

Materials and methods

Construction design of the air-assisted mechanical hill-seeding device

Agronomic requirements for foxtail millet planting specify a hill spacing of 160 ± 20 mm, a seeding depth of 30 to 50 mm, and 2 to 3 foxtail millet seeds per hole. Because the ground is initially covered with a layer of the plastic film prior to sowing, a spring duckbill device is installed around the periphery of the air-assisted mechanical foxtail millet seeding device to penetrate both the plastic film and the soil, thereby releasing the seeds. The structure of this air-assisted precision hill-seeding device for foxtail millet is depicted in Figure 1. The housing of the hill-seeding device is affixed to the revolving shaft; the external dibber wheel, rolling along the ground, drives the seed distributor to rotate through gear transmission. Within the device, an inner and outer disc are interconnected, creating a sealed seeding chamber. The seed box is mounted on the outer disc and is in communication with the seeding chamber, while a roller bearing on the outer disc ensures the relative rotation between the outer ring and the inner disc. Uniformly distributed between the outer ring and inner disc are seed receptacles that are in communication with the spring duckbill device.

During the operation of the hill-seeding device, the air holes of the air chamber are subjected to negative pressure, and the seeds in the filling area are loaded into the shaped holes under the influence of their gravitational force, inter-seed interaction, and negative pressure. With the rotation of the seed distribution disc, the seeds, influenced by the centrifugal force and their gravity, fall into the receiving box and enter the spring duckbill device. As the duckbill wheel rotates, the duckbill upper jaw first contacts the ground and penetrates the soil, and then the pressure plate makes contact with and revolves around the fixed pin, causing the duckbill to open to a predetermined size for seeding. Simultaneously, the return spring is compressed. Owing to the force of the spring, when the pressure plate leaves the ground, the duckbill closes (Chen et al., 2021). The seeding machine continues to move forward, and this process is repeated until the seeding is completed.

Determination of dibber wheel dimensions

The diameter of the dibber wheel, a critical parameter for determining the overall structure of the hill-seeding device, is related to the number of duckbills, the agronomic requirements for plant spacing, and the working speed of the seeding machine. The larger the diameter of the dibber wheel, the larger the diameter of the internal seed distributor of the hill-seeding device, which is conducive to seed filling, cleaning, and sowing. Additionally, the larger the diameter of the dibber wheel, the greater the overall mass of the seeding machine, promoting duckbill penetration into the soil. However, an excessively large diameter of the dibber wheel, with unaltered hole spacing, can lead to an increase in the number of duckbills, raising costs. Generally, the roller diameter of the duckbill roller seed distributor ranges from 360 to 480 mm, and the number of duckbills is typically even. In this study, considering a foxtail millet plant spacing of 160 mm, we chose 10 duckbills and set the roller diameter, D, at 450 mm.

Determination of duckbill hole-forming device dimensions

The larger the opening of the duckbill hole-forming device, the more conducive it is for the seeds to fall into the duckbill. In this study, the opening size of the duckbill hole-forming device was set at 36 × 36 mm (shown in Figure 2). As shown in Figure 3, under ideal working conditions, no relative slippage should occur between the hill-seeding device and the ground during contact. The theoretical plant spacings should be equal to the arc length corresponding to the angle between adjacent duckbills, making the theoretical plant spacing 160 mm. Given that the number of duckbills is fixed at 10 and the roller radius is 450 mm, Equation (1) yields R_2 = 500 mm:

$$s = \frac{\beta}{180}\pi R_2 = \frac{2\pi}{M}R_2 , \qquad (1)$$

where s is theoretical plant spacing, mm; β is the arc length corresponding to the angle between adjacent duckbills, mm; M is the number of duckbills; R_1 is the radius of the outer circle of the seed-metering device, mm; and R_2 is the duckbill tip track circle radius, mm.

The height of the duckbill in the dibber primarily depends on the foxtail millet sowing depth (h), with agronomic requirements stipulating a sowing depth of 30 to 50 mm. According to Equation (2), the calculated foxtail millet sowing depth is h = 50 mm, consistent with agronomic sowing requirements. The duckbill height, (H), is determined by the sowing depth; thus, H = h = 50 mm.

$$h = R_2 - R_1 . \qquad (2)$$

Determination of return spring parameters

The duckbill hole-forming device employs a conical spring, enabling the movement of the duckbill in a manner that minimizes the likelihood of clogging. However, during hole formation, the pressure plate is subjected to pressure from the soil, generating an opposite force. This force can place considerable stress on the mulch, resulting in severe damage or significant deformation, from which the mulch cannot recover. To reduce the force exerted on the mulch by the pressure plate and to ensure that the stress on the mulch is minimized while allowing the duckbill to complete the sowing, we select a spring with a smaller elastic coefficient (i.e., a spring with a smaller wire diameter), as shown in Figure 4. Based on the roller's width, the spring's larger diameter is chosen to be 44 mm, and the smaller diameter is 22 mm. The wire diameter of the spring generally ranges from 1.4 to 1.8 mm (Gu *et al.*, 2010). Considering the overall structure of the former hole and the size of the pressure plate, the spring must just contact the pressure plate without being compressed by it, remaining in a natural state. The length of the spring, L', is 500 mm. To ensure that the spring does not leak seeds before the pressure tongue plate contacts the surface owing to an excessively large elastic coefficient, we design a certain pre-deformation of the spring. Before the duckbill comes into contact with the soil, the maximum force exerted on the spring is the weight of the pressure plate, which weighs 0.126 kg, corresponding to a force P_1 = 1.235 N. Based on Equations (3) and (4), the deformation of the spring, ΔL, is calculated as 11.57 mm, and L_{min} = 61.57 mm. To ensure the working quality of the spring, we round up the spring length to L = 70 mm.

$$\Delta L = \frac{16P_1(R_3^2 + R_4^2)(R_3 + R_4)}{Gd^4}, \quad (3)$$

$$L_{\min} = \Delta L + L', \quad (4)$$

where P_1 is the force of the pressure plate against the return spring, N; G is the shear modulus of spring material, MPa. When the spring material is carbon steel, G = 79,000 MPa; when the spring material is stainless steel, G = 71,000 MPa. d is the spring wire diameter, mm; R_3 and R_4 are half of the small-end middle diameter and half of the big-end middle diameter of the spring, respectively, mm; ΔL is the deformation of the spring, mm; L_{min} is the minimum spring length, mm; and L' is the natural length of the spring, mm.

Bench test

Return spring performance test

To analyze the influence of the spring wire diameter on experimental indicators such as the sowing qualification rate, resowing rate, missing sowing rate, average seed distance, and seed distance variation index, and to determine the optimal diameter of the spring, we constructed an experimental platform, as shown in Figure 5. The conical springs had a height of 70 mm, a large-end diameter of 44 mm, a small-end diameter of 22 mm, and wire diameters of 14, 16, and 18 mm. The experiment focused on the "Jingu 21" grain variety. The grains were rinsed three times with water at around 50°C to remove a large amount of floating grain husks from the seed group. After treatment, the grains were air-dried for 3 days to achieve a moisture content of approximately 8%.

Owing to the near-rigid contact between the dibber and the conveyor belt, the vibration is large under high-speed test conditions, making it impossible to obtain reliable experimental data. Therefore, the conveyor belt speed was set at 0.46 m/s (3 km/h), equivalent to a dibber device rotational speed of 37 r/min. The number of grains in each dibber and the distance between adjacent dibbers on the conveyor belt were recorded to complete the comprehensive performance testing of the sowing device. Three sets of measurements were taken for each type of spring, with each set comprising 100 dibbers.

Negative pressure and rotational speed of dibber wheel tests

To study the effects of dibber device rotation speed and inlet negative pressure on the sowing qualification rate, resowing rate, missing sowing rate, average seed distance, seed distance variation index, and other experimental indicators, we constructed a testing apparatus, as shown in Figure 6. A vacuum was created by an air compressor through a vacuum generator, and the negative pressure at the air chamber inlet was controlled by adjusting the IRV10-C06 vacuum pressure regulating valve (Wenzhou, Zhejiang). The variable-speed electric motor was then activated, and the sowing device's rotational speed was measured using a SW-6234C type laser digital tachometer (Suwei, Guangzhou, Guangdong). Design-Expert 8.0 software was employed to design a two-factor, three-level experiment using negative pressure and speed as factors and to analyze the response of the quality index, Y_1, multiples index, Y_2, and miss index, Y_3, to experimental factors using the quadratic regression response surface methodology (RSM). The factor level coding table is shown in Table 1. The variety and treatment of the grain seeds were the same as in Section 2.2.1.

The response variable could be fitted into the general form of a quadratic polynomial model, and the equation can be expressed as (Bu *et al.*, 2020)

$$Y = \beta_0 + \sum_{i=1}^{3}\beta_i X_i + \sum_{i=1}^{3}\beta_{ii} X_i^2 + \sum_{i=1}^{2}\sum_{j=i+1}^{3}\beta_{ij} X_i X_j \quad , \qquad (5)$$

where Y is the response variable measured for each combination of factorial level; β_0, β_i, β_{ii}, β_{ij} are terms of regression coefficients for the intercept, linearity, square, and interaction, respectively.

Performance indicators

According to the industry standard DG/T007-2019 for multi-grain dibbling machinery equipment, issued by the Ministry of Agriculture and Rural Affairs of the People's Republic of China, the qualification rate of the dibbling machine's grain number per dibble must be ≥ 85%, and the qualification rate of dibble distance must be ≥ 90%. This study mainly considered the missing sowing rate, resowing rate, seed distance qualification rate, and seed distance variation coefficient as performance indicators for grain seeds, with two to three grains per dibble being acceptable; fewer than two grains considered missing sowing, and more than three grains considered resowing. Thus, when two to three seeds were discharged from the discharge spout, we counted this as “normal.” If there were fewer than two discharged seeds, it was counted as “miss,” and discharging more than three seeds at a time was counted as “multiple.” Moreover, the qualification for seed distance was 17 cm ± 2cm. The methods to evaluate the various performance indicators of the dibbling device are as follows:

$$I_C = \frac{Z_1}{Z} \times 100\% \quad , \qquad (6)$$

$$I_L = \frac{Z_2}{Z} \times 100\% \quad , \qquad (7)$$

$$I_H = 1 - I_L - I_C \quad , \qquad (8)$$

$$I_J = \frac{x}{X_r} \times 100\% \quad , \qquad (9)$$

$$\overline{X} = \frac{\sum_{i=1}^{n} x_i}{n} \quad , \qquad (10)$$

$$\sigma = \sqrt{\frac{\sum_{i=1}^{n}(x_i - \overline{X})^2}{n-1}} \quad , \qquad (11)$$

$$CV = \frac{\sigma}{\overline{X}} \times 100\% \quad , \qquad (12)$$

where I_C is the multiples index; I_L is the miss index; I_H is the quality index; Z is the number of total seed discharges; Z_1 and Z_2 are the counts of multiples and misses, respectively; I_J is the seed distance quality index; x is the measured seed distance, mm; X_r is the theoretical seed distance, mm; $\overline{X}$ is the mean seed distance, mm; n is total number of seed distance measurements; σ is the standard deviation of the seed distance; and CV is the coefficient of variation of the seed distance.

Results and Discussion

The influence of return spring wire diameter on seeding

As shown in Table 2, the experimental results show that setting the seeder's forward speed to 0.46 m/s (3 km/h), corresponding to a hole-forming device rotation speed of 37 r/min, led to no substantial variations in the sowing effect for springs with wire diameters of 1.4, 1.6, and 1.8 mm. All tested parameters met the sowing requirements. Under the precondition of opening the duckbill for seeding, minimizing the force on the film was achieved by selecting springs with a lower elastic modulus, specifically by choosing a wire diameter of 1.4 mm (Gu *et al*., 2010). The results show a seeding qualification rate of 87.00%, a replanting rate of 2.67%, a leakage rate of 10.33%, a grain distance qualification rate of 100%, an average grain distance of 16.45 mm, and a grain distance coefficient of variation of 2.69%.

3.2 Impact of negative pressure and dibber wheel rotation speed on seeding effectiveness

Using various factor-level code values as independent variables, with the quality index (Y_1), multiples index, (Y_2), and miss index (Y_3) as responses, we present the experimental results in Table 3, which lists qualification rates ranging from 85.67 to 92.00%, replanting rates from 1.33 to 2.33%, and leakage rates from 7.33 to 12.67%.

Utilizing Design-Expert 8.0 software, we conducted a multivariate regression analysis of the experimental results. This investigation aimed to elucidate the effects of various influencing factors on the quality index (Y_1), multiples index (Y_2), and miss index (Y_3) through an analysis of variance (ANOVA). The significance levels for each influencing factor were determined using p-values, and multivariate regression equations were utilized to model the functional relationships between factors and responses. Bivariate regression equations for the quality index (Y_1), multiples index (Y_2), and miss index (Y_3) were obtained, and the interactive effects of each factor on the response were elucidated through a response surface analysis.

(1) Response surface analysis of quality index, Y_1

The response variance analysis for the qualification rate is presented in Table 4. The regression model for the qualification rate was found to be significant ($P < 0.05$), indicating meaningfulness in the regression equation. With a lack of fit $P > 0.05$, the regression equation demonstrated good fit and possessed practical relevance. The results reveal significant factors ($P < 0.05$) influencing the leakage rate, namely X_1, X_2, and the interaction term X_1X_2. The contributing influence of these factors, in descending order, was the negative pressure at the air intake and the rotation speed of the hole-forming device. Thus, the regression model for the quality index, Y_1, was obtained as follows:

$$Y_1 = 90.46 + 1.33X_1 - 1.45X_2 + 1.25X_1X_2 - 0.61X_1^2 - 0.61X_2^2 \quad (13)$$

A response surface analysis was utilized to investigate the interactive effects of the inlet negative pressure and dibber wheel rotation speed on the quality index. As can be seen from Figure 7, the interaction between the inlet negative pressure and dibber wheel rotation speed had a noticeable impact on the quality index. With the dibber wheel rotation speed fixed, the quality index initially increased and then decreased as the inlet negative pressure increased. This trend was not pronounced because the key seeding component inside the dibber wheel is a mechanically operated hole-type seeder, and the inlet negative pressure assists in mechanical filling by applying negative pressure. When the dibber wheel rotation speed was fixed, the auxiliary air pressure could provide a favorable assisted filling effect within a certain level range. With the inlet negative pressure fixed within a reasonable range, as the dibber wheel rotation speed increased, the quality index significantly decreased. This decrease is attributed to the excessive centrifugal force generated by an overly high dibber wheel rotation speed. An excessive centrifugal force can negatively affect the filling quality, leading to a decline in the quality index. Conversely, the lower the dibber wheel rotation speed, the better the seeding effect.

(2) Response surface analysis of multiples index (Y_2)

The ANOVA results for the multiples index are shown in Table 5. The results show that X_1 and X_2 and their interaction did not have a significant effect on the multiples index. During the experiment, given a dibber wheel rotation speed, reducing the inlet negative pressure diminished the suction on the seeds during the filling process, leading to an increase in the miss rate. However, increasing the inlet negative pressure only increased the qualification rate, due to the size limitations of the hole, which did not permit more than three seeds to enter each hole. Similarly, given an inlet negative pressure, reducing the dibber wheel rotation speed could improve the filling effect and increase the qualification rate, but again, no more than three seeds could enter each hole. Increasing the dibber wheel rotation speed would lead to an increased miss index due to factors like higher centrifugal force and reduced filling time. Therefore, the negative pressure at the inlet and the rotation speed of the dibber wheel did not have a significant impact on the multiples index in this experiment.

(3) Response surface analysis of miss index, Y_3

The ANOVA for the miss index response is presented in Table 6. The regression model for the acceptance rate demonstrated significance with $P < 0.05$, rendering the regression equation meaningful. Furthermore, with the lack-of-fit value $P > 0.05$, the regression equation exhibited an excellent fit and carried substantive practical significance. The results reveal that concerning the miss rate, X_1, X_2, X_1X_2, and X_2^2 were significant factors ($P < 0.05$), with the contribution rate of the negative pressure at the air intake and the rotational speed of the dibber being consistent. The regression model describing the relationship between these factors and the response is as follows:

$$Y_3 = 7.73 - 1.22X_1 + 1.22X_2 - 1.25X_1X_2 + 0.76X_1^2 + 0.76X_2^2 \quad . \qquad (14)$$

As shown in Figure 8, the interaction between the negative pressure at the air intake and the dibber rotational speed had a noticeable impact on the miss index. With the dibber rotational speed fixed, it can be observed that as the negative pressure at the air intake increased, the acceptance rate first decreased and then increased, although the trend was not pronounced. When the negative pressure at the air intake was within a specific range and fixed, it can be seen that as the dibber rotational speed increased, the miss index significantly increased.

To enhance the seeding efficiency, we conducted parameter optimization through a response surface analysis, targeting the maximum quality, minimum multiples, and miss indexes. Validation experiments were performed on the optimized results using identical test materials, comprising three sets with a total of 300 seeds each. The optimization and validation experiment results are depicted in Table 7. When the negative pressure at the air intake was −7.8 kPa, and the dibber rotational speed was 75 r/min, corresponding to a seeder forward speed of 1.69 m/s (6.08 km/h), the quality index was 89.88%, the multiples index was 1.56%, and the miss index was 8.56%. These results demonstrate that the optimal level combination tailored for the quality index, multiples index, and miss index met the design requirements. The discrepancy between the bench test results and predictions is less than 10%, consistent with preliminary experimental conclusions, thus providing a theoretical basis for further research.

Field experiment verification

On May 8, 2021, an experiment was conducted in the experimental fields of the School of Mechanical and Electrical Engineering at Northwest A&F University in Xianyang, China. Three foxtail millet hill-seeding devices were mounted on the base frame in parallel to maintain an inter-row distance of 300 mm. Prior to the experiment, rotary tilling was performed to level the field. After preparation, a 20-m-long seeding area was marked, and the seeder completed two rows in a single back-and-forth journey at a sampling machine speed of 1.67 m/s (6 km/h) and an inlet negative pressure of −7.8 kPa. The field experiment process is shown in Figure 9.

Group ①, with stable seeding quality among 18 holes in each row, was selected as the field experiment measurement area. The quality index, multiples index, miss index, seed distance quality index, mean seed distance, and the coefficient of variation of seed distance were statistically analyzed and calculated. Within the three rows of seeding in group ①, 30 consecutive measurements were randomly selected for each row. The results are presented in Table 8.

The experimental results show that when the seeding machine advanced at a speed of 1.67 m/s (6 km/h) with an inlet negative pressure of −7.8 kPa, the average seeding qualification rate was 88.46%, with a 100% hole spacing qualification rate, an average grain distance of 16.51 mm, and a hole spacing coefficient of variation of 2.55%. These findings meet the DG/T007-2019 industry standard for seeding machines.

Compared to the foxtail millet drill seed-metering device (Yang *et al.*, 2020), the air-assisted mechanical foxtail millet hill-seeding device could precisely control the seeding amount. It exhibits a seeding qualification rate comparable to the suction type millet precision seed meter (Zhu *et al.*, 2023), while demonstrating a significant advantage in hole spacing qualification rate. Similar findings were reported in studies on lettuce (*Latuca sativa L.*) planters. Siemens and Gayler (2016) found that the seed spacing performance of belt planters was significantly better than vacuum planters, especially at higher speeds. The underlying cause of this phenomenon is the seed release height, indicating that lower seed drop height and control of seed trajectory patterns are crucial factors in hole spacing control (Parish and Bracy, 2003; Panning *et al.*, 2000). Therefore, precision hill-seeding devices show potential in both grain and vegetable sowing.

The foxtail millet seedling emergence on May 18, 2021, is depicted in Figure 10. In the group labeled ②, where the seeding quality was stable, a stretch of 18 m between seeds was designated as the emergence rate measurement area. Statistics on its emergence rate were collected by randomly and continuously measuring 30 sets of data for each row, with the emergence numbers presented in Table

9. The emergence of one to three seedlings per hole was deemed acceptable, resulting in an overall seedling emergence qualification rate of 97.77%. This result complies with the design requirements of the DG/T007-2019 foxtail millet seeding machine standard.

Conclusions

To address the issue of suboptimal seeding efficiency for small foxtail millet seeds, we designed an air-assisted mechanical foxtail millet hill-seeding device and examined the effects of the duckbill hole-forming device's return spring wire diameter on the seeding quality, as well as the interactive impact of seed distributor negative pressure and dibber wheel rotational speed on the quality index. The findings are as follows. (1) When the return spring's major diameter was 44 mm, the minor diameter was 2 mm, and the length was 70 mm, the wire diameters were 1.4, 1.6, and 1.8 mm, respectively, and the quality index met the standard requirements. Considering that a smaller wire diameter results in lesser tearing of the membrane, a wire diameter of 1.4 mm was selected. (2) The seed distributor's negative pressure and dibber wheel rotational speed significantly influenced the quality index. Utilizing the RSM for parameter optimization, with maximum quality index, minimum miss index, and multiples index as the objectives, we found optimal conditions. Specifically, when the inlet negative pressure was −7.8 kPa, the dibber wheel speed was 75 r/min, the seeding machine's forward speed was 1.69 m/s (6.08 km/h), the quality index was 89.88%, the multiples index was 1.56%, and the miss index was 8.56%, consistent with the model's predictions. Following the determination of these parameters, field trials were conducted. The test results show that at a seeding machine forward speed of 1.67 m/s (6 km/h) and a seed distributor negative pressure of −7.8 kPa, the average grain spacing was 16.51 mm, the hole spacing coefficient of variation was 2.55%, the average seeding quality index was 88.46%, and the seedling qualification rate was 97.77%. Thus, the designed foxtail millet seeding machine complies with the standard requirements. These findings could provide relevant theoretical and technical support for improving the reliability of foxtail millet planter.

References

Bian, Y., Ma, Y., Zhang, Z., 2007. Reciprocating feeder applied to precision seed-grain sowing machines. Transactions of the Chinese Society for Agricultural Machinery 23, 122-127.

Bu, L., Hu, G., Chen, C., Sugirbay, A., Chen, J., 2020. Experimental and simulation analysis of optimum picking patterns for robotic apple harvesting. Sci Hortic-amsterdam 261, 108937.

Chen, Y., Cheng, Y., Chen, J., Zheng, Z., Hu, C., Cao, J., 2021. Design and experiment of the buckwheat hill-drop planter hole forming device. Agriculture 11, 1085.

Cui, Q., Qin, G., Wang, M., 2003. The analysis and comparison on several kinds of precision feed

mechanism. Journal of Shanxi Agricultural University (Natural Science Edition) 23, 69-71.
Gu, F., Hu, Z., Wang, H., Ji, F., Tian, L., 2010. Design of a duck bill-roller peanut seeder and analysis of its trajectory. Chinese Agricultural Mechanization 4, 60-63.
Kang, S., Ni, X., Qi, Q., Li, S., Xu, G., 2020. Design and experiment of pneumatic cylinder precision seed-metering device for cotton. Journal of Agricultural Mechanization Research 42, 136-141.
Li, N., Zhao, M., Liu, F., Liu, Y., Lv, B., Zhang, T., Dong, S., Chen, C., 2016. Experimental study on the performence of pheumatic precision metering device for foxtail millet seeds. Journal of China Agricultural University 21, 122-128.
Panning, J.W., Kocher, M.F., Smith, J.A., Kachman, S.D., 2000. Laboratory and field testing of seed spacing uniformity for sugarbeet planters. Applied Engineering in Agriculture 16, 7-13.
Parish, R.L., 1972. Development of a narrow-row, vertical-plate planter. T Asae 15, 636-0637.
Parish, R., Bracy, R., 2003. An attempt to improve uniformity of a Gaspardo precision seeder. HortTechnology 13, 100-103.
Siemens, M.C., Gayler, R.R., 2016. Improving seed spacing uniformity of precision vegetable planters. Applied Engineering in Agriculture 32, 579-587.
Singh, R.C., Singh, G., Saraswat, D.C., 2005. Optimisation of design and operational parameters of a pneumatic seed metering device for planting cottonseeds. Biosystems Engineering 92, 429-438.
Wan, L., Wang, H., Che, G., 2019. Design and test of rice hill-drop seed metering device embedded with rotating air cavity. Transactions of the Chinese Society of Agricultural Machinery 50, 74-84.
Xie, W., Liu, Y., 2018. Seeding performance of rape seeding device of socket-roller. Contemporary Farm Machinery, 67-69.
Yang, H., Zhao, D., 2007. Research present situation and tendency about performance examination way of foxtail millet precision seeder. Journal of Agricultural Mechanization Research 2, 34-35.
Yang, Z., Zhang, Y., Wang, H., Yi, S., Guo, S., Ma, Y., 2020. Experimental study on seeding performance of the millet drill seed-metering device. Journal of Agricultural Mechanization Research 42, 197-202, 213.
Zhang, X., Shan, L., Li, Z., Wang, L., Chai, Y., 2007. The production and distribution of minor crops in the Loess Plateau of China. Chinese Journal of Eco-Agriculture 15, 80-85.
Zhang, Y., Liu, F., Zhao, M., Lv, B., 2016. Small size Air-suction seed seedmeter suction hole cleaning device design and simulation. Journal of Agricultural Mechanization Research 38, 23-27.
Zhang, Y., Zhang, W., Li, D., 2010. Design for precision metering device with center transmission. Transactions of the Chinese Society for Agricultural Machinery 41, 78-81+121.
Zhu, J., Liu, J., Fu, Y., Xi, Y., 2023. Design and experiment of a suction type millet precision seed

meter. Journal of Hebei Agricultural University 46, 111-117.

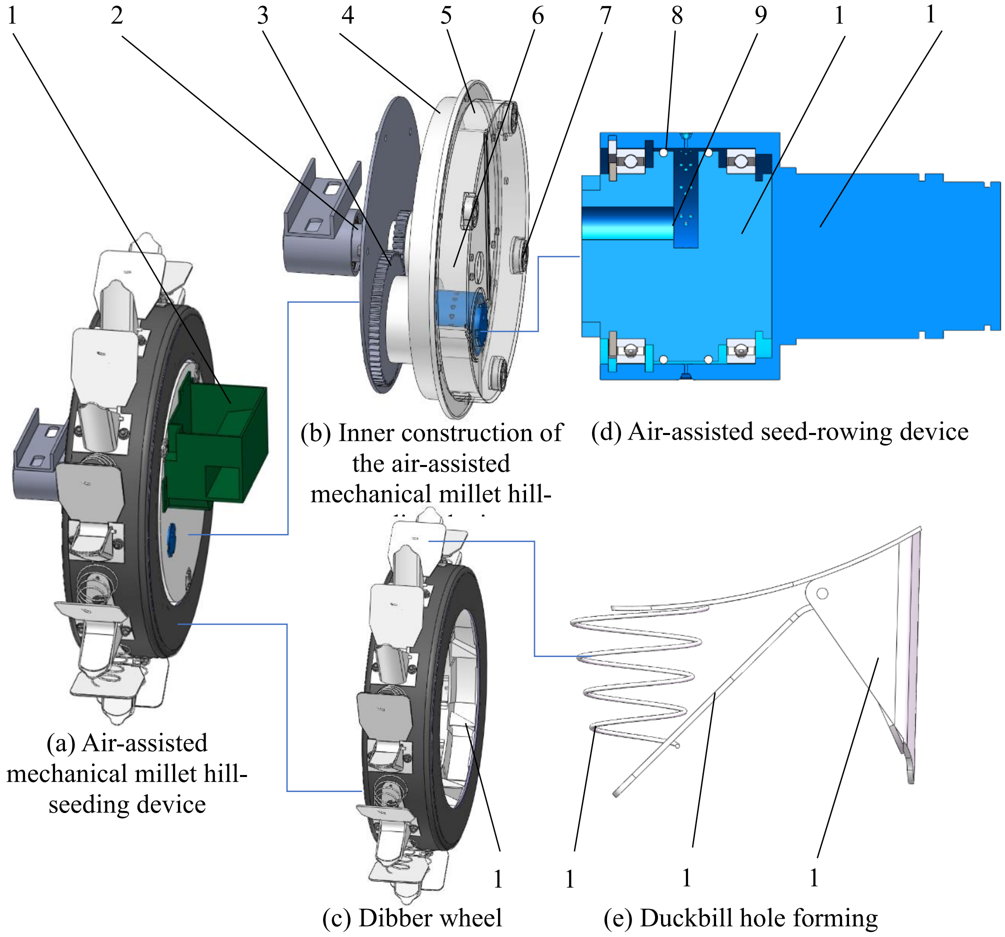

Figure 1. Structure schematic diagram of the air-assisted mechanical foxtail millet hill-seeding device: (1) seed box, (2) revolving shaft, (3) transmission gear, (4) inner disc, (5) outer disc, (6) seed filling area, (7) idler wheel, (8) sealing ring, (9) air chamber, (10) stator, (11) rotor, (12) seed receiving box, (13) return spring, (14) pressure plate, and (15) duckbill upper jaw.

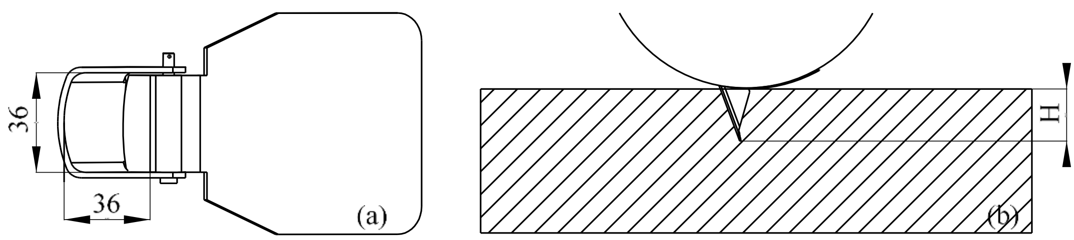

Figure 2. Structure drawing of the cavitation device: (a) the bottom surface of the hole-forming device and (b) diagram of the depth of the hole-forming device.

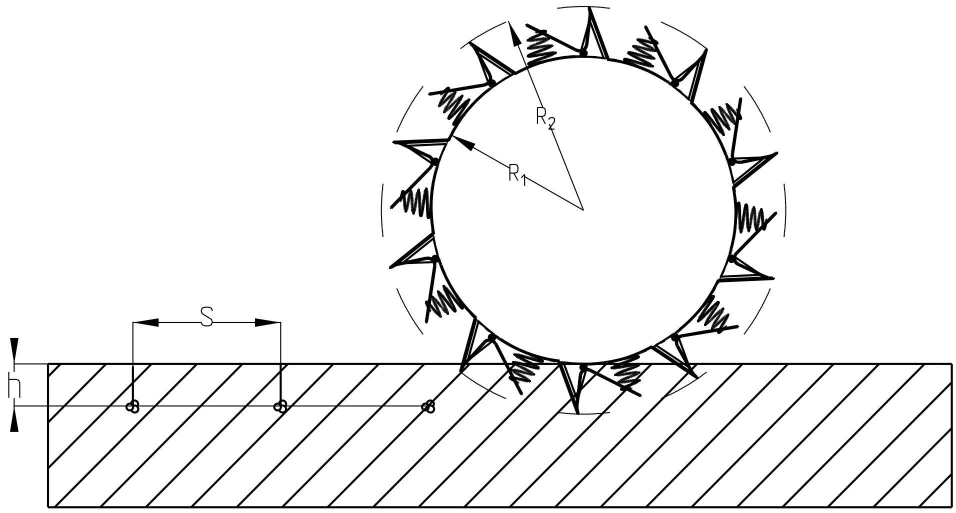

Figure 3. Structure of air-suction auxiliary mechanical grain hill seeder.

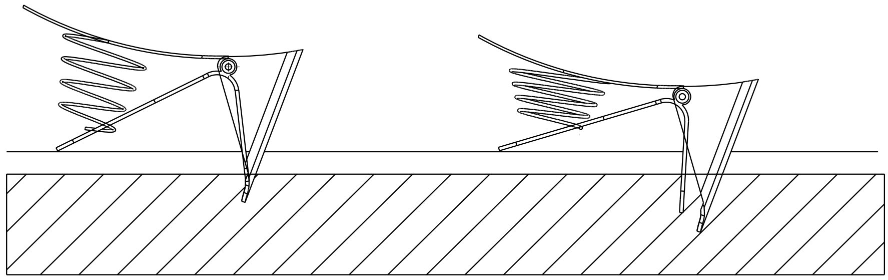

Figure 4. Working state of the duckbill hole-forming device.

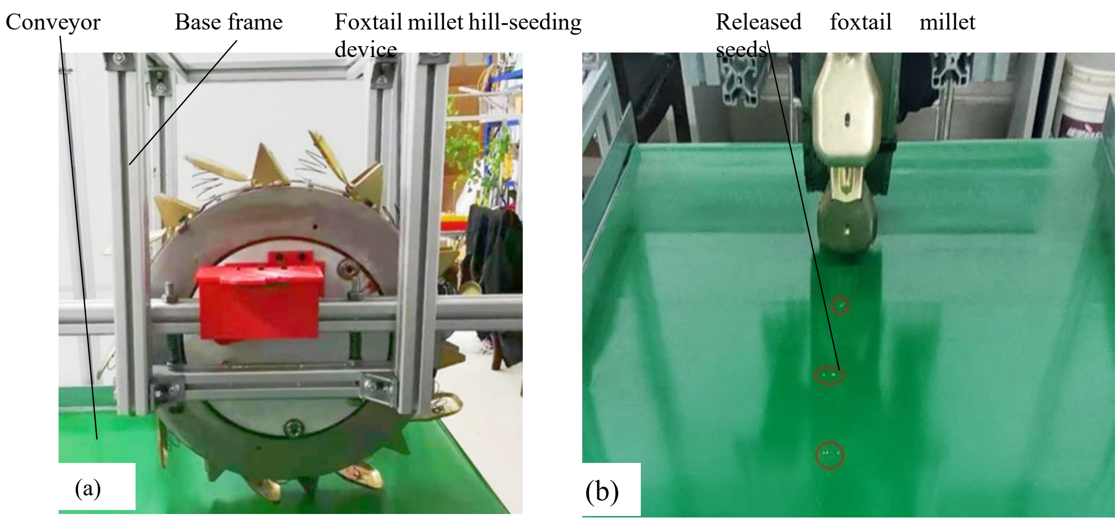

Figure 5. Table test of air-assisted mechanical hill seeder: (a) installation diagram of hill

seeder and (b) result diagram of hill-seeder seed arrangement test.

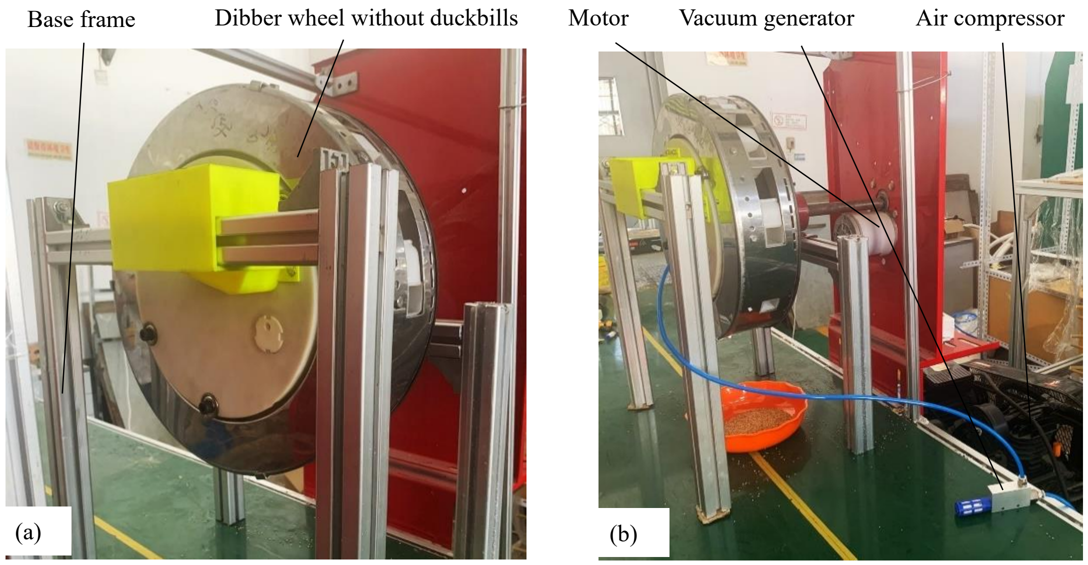

Figure 6. Table test of air-assisted mechanical hill seeder: (a) diagram of hill-seeder bench installation and (b) seed arrangement performance test chart of hill seeder.

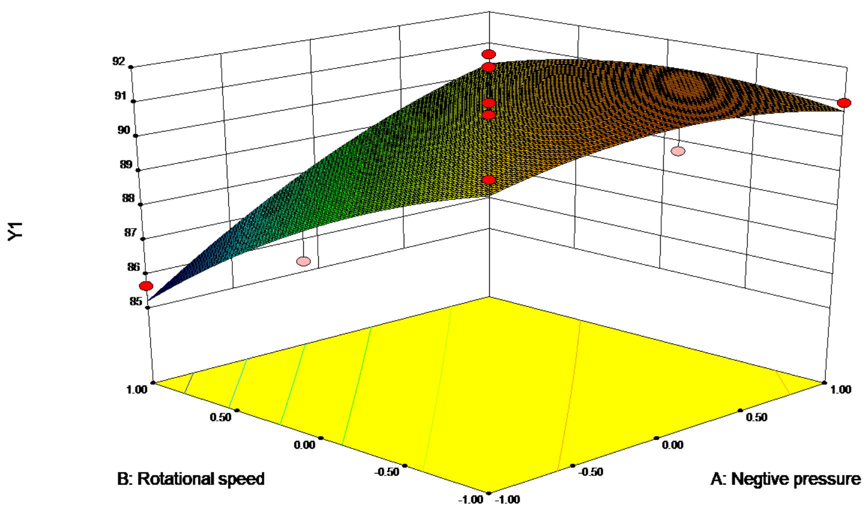

Figure 7. Contour and surface plots of the negative pressure and rotation speed effects on the predicted responses.

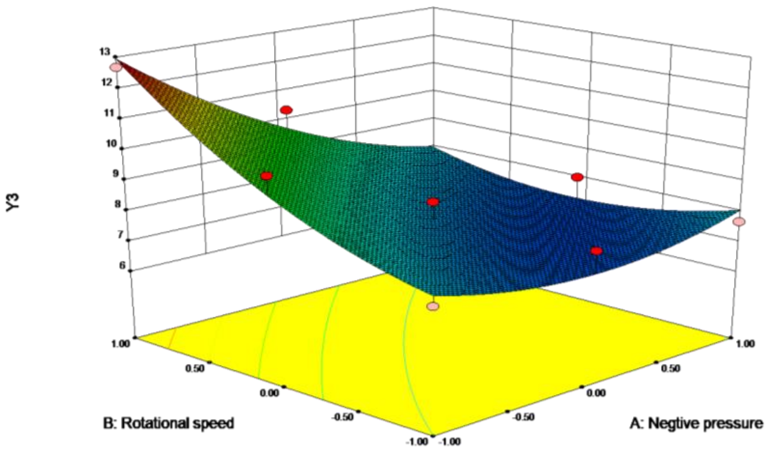

Figure 8. Contour and surface plots of the negative pressure and rotation speed effects on the predicted responses.

Figure 9. Field test: (a) seeding in progress and (b) Operation effect of seeder after seeding.

Figure 10. Foxtail millet seedling emergence.

Table 1. Experimental factors and level code

Factors	Unit	-1	0	1
Negative Pressure (X1)	-kPa	7.0	8.0	9.0
Rotational speed of dibber wheel (X2)	r/min	75	80	85

Table 2. Comprehensive performance test results of hill seeder

Return spring wire diameter (mm)	Conveyor line speed (km/h)	Quality index (%)	Multiples index (%)	Miss index (%)	Quality index for seed distance (%)	Mean seed distance (cm)	Standard deviation of seed distance	Coefficient of variation of seed distance (%)
1.4	3	87.00	2.67	10.33	100	16.57	4.4478	2.69
1.6	3	86.66	2.67	10.67	100	16.62	3.8388	2.31
1.8	3	87.67	3.00	9.33	100	16.44	4.6751	2.84

Table 3. Experimental design made up of two independent variables at three levels, and the results of the responses.

	Negative Pressure X1	Rotational speed X2	Quality index Y1 (%)	Multiples index Y2 (%)	Miss index Y3 (%)
1	0	0	91.00	1.67	7.33
2	0	−1	90.67	1.33	8.00
3	0	1	87.67	2.00	10.33
4	−1	1	85.66	1.67	12.67
5	−1	−1	91.00	1.33	7.67
6	0	0	90.66	1.67	7.67
7	1	−1	91.00	1.33	7.67
8	1	0	90.67	1.33	8.00
9	0	0	92.00	1.33	6.67
10	−1	0	87.67	2.00	10.33
11	0	0	90.34	2.33	7.33
12	0	0	89.67	2.00	8.33
13	1	1	90.66	1.67	7.67

Table 4. ANOVA of model response to quality index.

Source	Sum of Squares	DOF	Mean Square	F-value	p-value
Model	32.881	5	6.56	7.99	0.0082**
X1	10.67	1	10.67	13.00	0.0087**
X2	12.56	1	12.56	15.30	0.0058**
X1X2	6.25	1	6.25	7.61	0.0281*
X12	1.03	1	1.03	1.26	0.2993
X22	1.03	1	1.03	1.26	0.2993
Residual	5.77	7	0.82		
Lack of fit	2.79	3	0.93	1.25	0.4030
Pure Error	2.97	4	0.74		

Table 5. ANOVA of model response to multiples index.

Source	Sum of Squares	DOF	Mean Square	F-value	p-value
Model	0.580	5	0.120	1.06	0.4537
X1	0.075	1	0.075	0.69	0.4345
X2	0.300	1	0.300	2.79	0.1388
X1 X2	-1.11E-16	1	−1.11E-16	−1.02E-15	1.0000
X12	0.062	1	0.062	0.57	0.4761
X22	0.062	1	0.062	0.57	0.4761
Residual	0.760	7	0.110		
Lack of fit	0.190	3	0.062	0.43	0.7417
Pure Error	0.580	4	0.140		

Table 6. ANOVA of model response to miss index.

Source	Sum of Squares	DOF	Mean Square	F-value	p-value
Model	29.32	5	5.86	10.05	0.0043**
X1	8.95	1	8.95	15.35	0.0058**
X2	8.95	1	8.95	15.35	0.0058**
X1 X2	6.25	1	6.25	10.71	0.0136*
X12	1.60	1	1.60	2.74	0.1420
X22	1.60	1	1.60	2.74	0.1420
Residual	4.08	7	0.58		
Lack of fit	2.63	3	0.88	2.400	0.2085
Pure Error	1.46	4	0.36		

Table 7. Comparison between predicted and test results.

	Negative pressure (-kPa)	Rotational speed (r/min)	Quality index (%)	Multiples index (%)	Miss index (%)
Predicted results	7.85	75	91.27	1.44	7.29
Experimental results	7.80	75	89.88	1.56	8.56

Table 8. Field test results.

Row number	Quality index (%)	Multiples index (%)	Miss index (%)	Seed distance quality index (%)	Coefficient of variation of seed distance (%)
1	90	3.33	6.67	100.00	2.67
2	86.66	6.67	6.67	100.00	2.55
3	83.34	3.33	13.33	100.00	2.42
Mean	86.67	4.45	8.89	100.00	2.55

Table 9. Statistical results of seedling emergence rate.

Row number	Seedling emergence rate (%)				
	0	1	2	3	>3
1	3.33	16.67	50.00	30.00	0
2	0	30.00	43.33	23.33	3.33
3	0	26.67	26.67	46.67	0
Mean	1.11	24.44	40.00	33.33	1.11
Total	1.11	97.77			1.11